Geo-loop: A Novel System for Characterizing Multiphase Flow of Saline Geothermal Fluids at Elevated Pressures and Temperatures

Adolph Bravo Jr., Andri Stefánsson, Erlend Straume, and Samuel Scott

Faculty of Earth Sciences, University of Iceland, 102 Reykjavik

ajm10@hi.is

Keywords: *Multiphase flow; Geothermal fluids; Fluid flow experiments; Flow loop*

ABSTRACT

The effective design, operation, and optimization of geothermal wells and surface facilities depend on the accurate understanding of multiphase flow. While extensive research has characterized such flows, most studies have been limited to near-ambient conditions using simplified systems like air–water or oil–gas. Applying these models to geothermal fluids with high temperatures, pressures, and salinities often leads to significant inaccuracies. This paper introduces Geo-loop, the first dedicated experimental facility designed to directly observe and investigate multiphase flow in geothermal fluids. The Geo-loop enables experiments at temperatures up to 200 °C, pressures up to 25 bar, and salinities up to 11 wt% NaCl. Equipped with an optical window and gamma densitometers, the system allows for direct visualization of flow regimes and precise void fraction measurements. These capabilities provide critical insights into multiphase flow under geothermal conditions and support the development of more accurate predictive models specifically for high-temperature, high-salinity systems.

1. INTRODUCTION

Conventional high-enthalpy geothermal fields typically operate with concurrent flow of multiple phases, specifically steam and brine. In some cases, multiphase transport occurs as early as within the reservoir and continues through the wellbore, surface piping, and into steam-brine separators. Managing multiphase flow has therefore been a key engineering challenge in the utilization and optimization of geothermal resources.

Strict analytical solutions to multiphase flow problems require prior knowledge of the distribution and geometry of the phases within the pipe. However, when multiple phases or components flow simultaneously, they can adopt a range of geometric and topological configurations, commonly referred to as flow regimes. Because these regimes must be predefined, applying strict analytical approaches becomes challenging. To implement an analytical approach in solving multiphase problems, it is therefore necessary to include constitutive models alongside the conservation laws of mass, energy, and momentum (Hewitt and Yadigaroglu 2017; Hasan and Kabir 2018). Constitutive models are particularly used to describe the relative motion between phases, often expressed in terms of void fraction, slip, or liquid holdup, and to estimate total frictional losses as well as other important characteristics of multiphase flow.

A wide range of constitutive correlations have been developed for multiphase flow modeling. Among these, those commonly applied in geothermal wellbore and pipe simulators include the correlations developed by Duns and Ros (1963), Orkiszewski (1967), and Rouhani and Axelsson (1970). Additional correlations are available and have been compiled in the reviews by Godbole et al. (2011), Yagidorlu et al. (2018), Márquez-Torres et al. (2020), and Ribeiro et al. (2020). These reviews highlight that most multiphase flow models have been developed using experimental data from air-water and oil-gas systems, most under ambient temperature conditions. However, recent investigations (Gokcal et al. 2008; Schmidt et al. 2008; Ribeiro et al. 2020; Al-Dogail and Gajbhiye 2021) have shown that fluid properties such as viscosity, density, and surface tension strongly influence multiphase flow behavior. These properties vary significantly with temperature and fluid composition, and can lead to flow regime transitions and interfacial dynamics under geothermal conditions that are not captured by conventional models. As a result, applying these models beyond their original experimental range can introduce substantial inaccuracies, highlighting the limitations of generalizing constitutive models outside their validated domains.

Despite these limitations, multiphase flow simulations, specifically in their applications in wellbore modeling, still play an important role in the design and operation of geothermal wells. For example, wellbore simulators have been used to design well completions that optimize production (King et al., 1995; Grant and Bixley, 2011). Various geothermal operators have also applied wellbore simulators to diagnose and address production decline caused by wellbore-related issues (Alvarez and Cinco, 2011; Libert and Alvarez, 2015; Kabigting et al., 2021). These examples highlight how wellbore simulators are invaluable tools for geothermal field management and decision making.

In most cases, wellbore simulators typically offer a selection of constitutive models from which the engineer must choose, leading to variations in results depending on the selected correlation (Tonkin et al. 2021). These variations in simulation outcomes may stem from the limited applicability of constitutive correlations beyond their original validation range, underscoring the importance of studying multiphase flow under geothermal-relevant conditions to ensure accurate flow characterization and improve model reliability.

In this paper, we present the Geo-Loop, the first dedicated flow loop specifically designed to investigate multiphase flow behavior in geothermal fluids. The system was developed by TWI Ltd. (Cambridge, UK) and assembled at the University of Iceland as part of the H2020 GeoPro project (Grant Agreement No. 851816). The Geo-Loop enables experiments at temperatures up to 200 °C, pressures up to 25 bar, and with NaCl concentrations ranging from 0–11wt% in the liquid phase. The system allows for direct visualization of flow regimes and measurements of bulk fluid density– parameters that are essential for the development of constitutive models. The system provides a platform both for

ISSN 2703-4275

evaluating existing correlations and for developing new ones that are better suited to geothermal conditions.

2. GEO-LOOP: DESIGN AND OPERATION

2.1 The Geo-loop setup

The Geo-Loop (Figure 1) consists of two main parts: the flow generation section and the test section. In the flow generation section, the test fluid is loaded and pumped, and experimental parameters such as pressure, temperature, fluid composition, and flow rates of each phase are controlled. In the test section, multiphase flow behavior is evaluated through flow regime observation and bulk fluid density measurements.

The design of Geo-loop allows for both vertical upwards and horizontal multiphase flow tests. Figure 1b demonstrates the configuration for vertical upwards tests. For horizontal flow experiments, the test pipe is rotated and repositioned accordingly, and the inlet and outlet are connected using prefabricated pipe sections.

A centralized control board (GeoPro control board, TWI Ltd.) integrates all electrical and mechanical components of the system, including inputs from transducers. It features a real-time user interface for monitoring system parameters and alarms. The board enables centralized control of experimental settings such as temperature and pump speed. Data from all transducers are collected by the board and transferred to a connected computer for storage and archival.

Flow generation section

Figure 2 shows the components of the flow generation section, including the reservoir, pump, rotameter, ultrasonic flowmeter, and various auxiliary valves.

The reservoir is a 33-L pressure vessel constructed by KW Group for the GeoPro project. In this vessel, the liquid phase, which is prepared by dissolving known amount of NaCl (S9888, Sigma-Aldrich) in deionized water, is loaded. The vessel is made from 316 stainless steel lined with Hastelloy C276. The vessel has two 1-inch ports, used as two-phase inlet at the top and liquid phase outlet at the base, and several 3/8-inch female NPT ports for gas phase outlet, pressure and temperature transducers, gas exhaust, rupture disc connections, and fluid loading inlet.

Temperature and pressure within the system are both controlled and monitored through the reservoir. Four electric heaters, mounted on the walls of the pressure vessel, operate independently and are automatically regulated, providing stable thermal conditions throughout the experiments. Pressure is manually adjusted by either introducing compressed nitrogen (UN1066, Linde) or carbon dioxide (UN1013, Linde) from pressurized cylinders or venting gas to the atmosphere. A single-stage regenerative turbine pump (STM 2.5x8.5, March May Ltd.) circulates fluid within the system. The pump has an adjustable speed, with a maximum flow rate of 116.7 L min^{-1}, and can tolerate some gas entrainment. As shown in Figure 2, the pump suction is connected to both the liquid and gas phase lines from the reservoir, allowing intake from both phases. The liquid-phase flow rate is measured externally using an ultrasonic flowmeter (KATflow 150, Katronic Technologies Ltd.), while the gas phase is monitored using a rotameter (MTG3809G, Brooks Instrument). To adjust the liquid and gas phase flow, the control valve (Figure 2b) is partially closed, which reduces liquid flow and enables more gas to be entrained through suction.

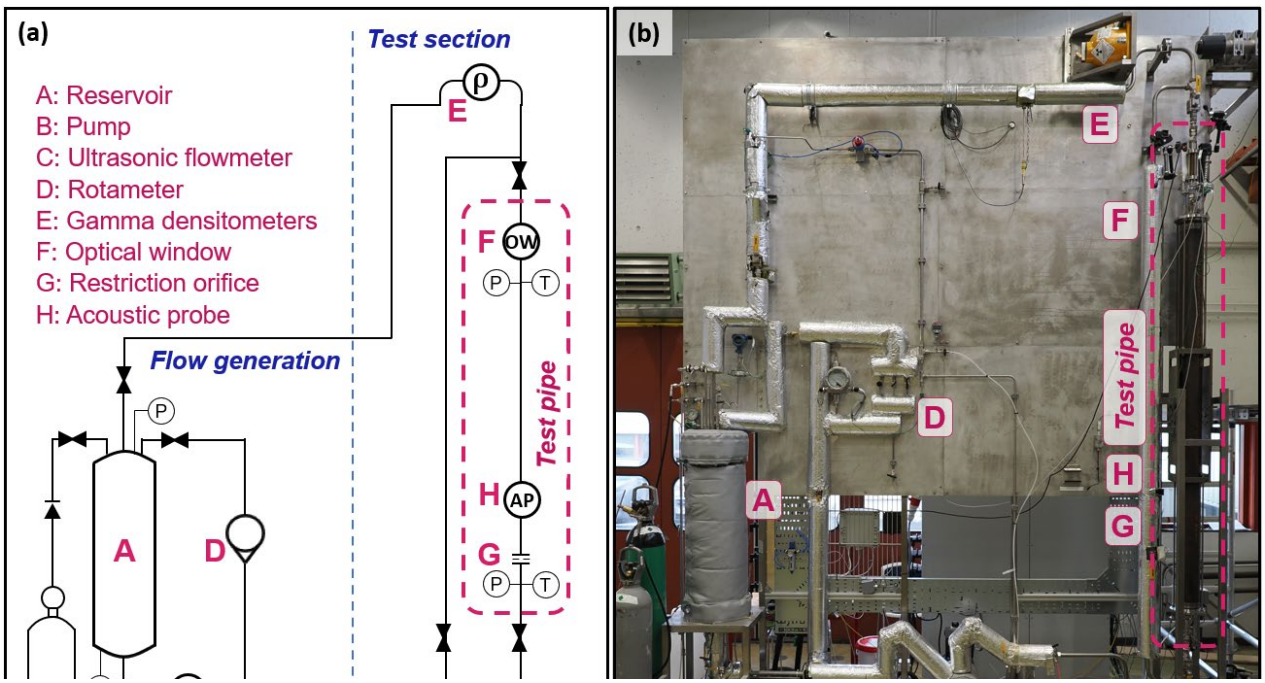

Figure 1. (a) Schematic diagram of the Geo-loop showing the main components, and (b) the system as installed at the University of Iceland in the vertical upward flow configuration. For horizontal flow experiments, the test pipe is repositioned and connected using prefabricated pipe segments.

ISSN 2703-4275

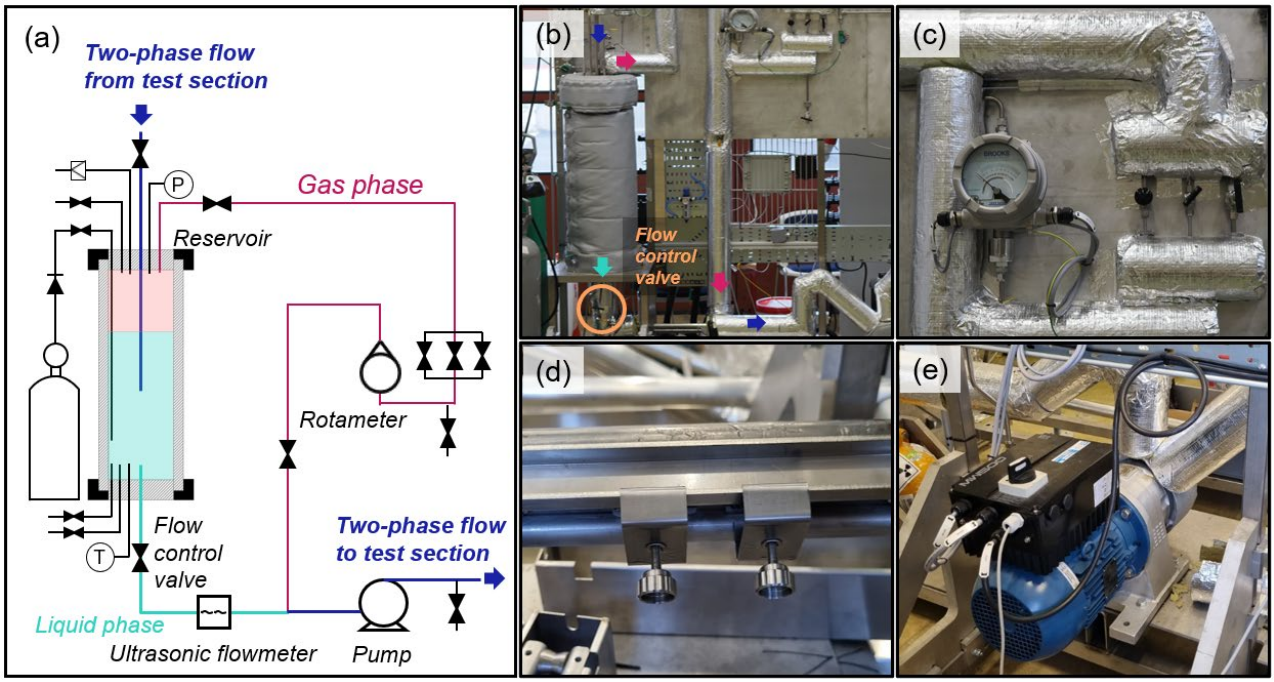

Figure 2. (a) Schematic diagram of the flow generation section showing the two-phase inlet and gas and liquid phase outlet streams, and actual installations of the (b) reservoir with the control valve, (c) rotameter, (d) ultrasonic flowmeter sensors, and (e) pump.

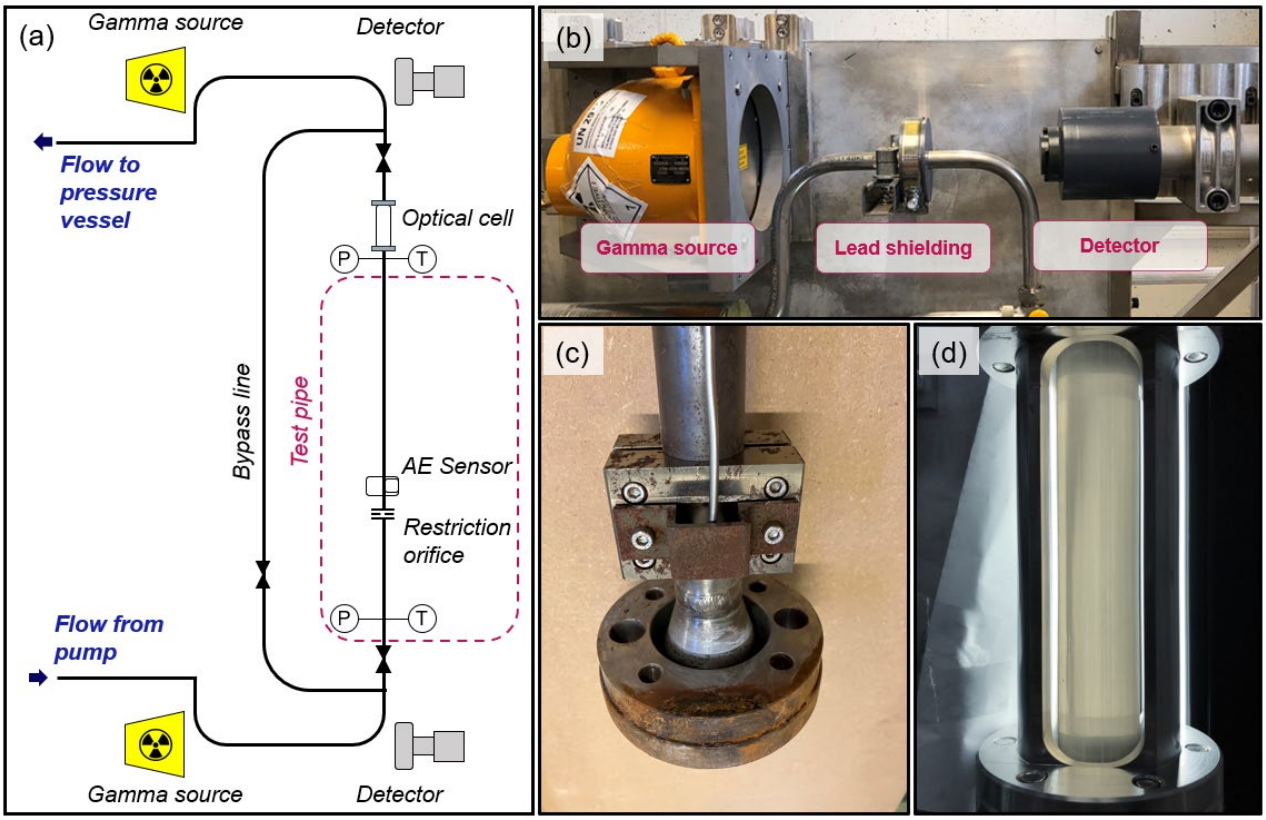

Figure 3. (a) Schematic diagram of the test section showing the equipment used to measure flow parameters, and actual installations of (b) the densitometer, (c) restriction orifice and acoustic emissions sensor, and (d) optical cell.

Proceedings 47th New Zealand Geothermal Workshop
11 -13 November 2025
Rotorua, New Zealand
ISSN 2703-4275

Test section

Figure 3 shows the test section, which consists of the test pipe, two gamma densitometers, an optical window, and an acoustic emission (AE) probe. The test pipe is composed of two straight segments connected by an orifice flange, with a total length of 2 meters. This straight configuration stabilizes the flow before it reaches the optical window. For horizontal tests, the test pipe is rotated into a horizontal orientation, and pre-fabricated pipe segments are attached to form an S-shaped configuration.

Bulk fluid density was continuously monitored at the inlet and outlet of the test section using two gamma densitometers (Berthold Technologies). Gamma densitometry determines fluid density by measuring radiation attenuation, which increases proportionally with density (Kumara et al., 2010; Vestøl et al., 2017), making it well suited for non-intrusive, real-time measurements in multiphase flow systems (Schmidt et al., 2008; Lv et al., 2014; Affonso et al., 2020). Each densitometer comprised a Cs-137 radiation source (2.22 GBq) and a Duo Series LB4700 NaI detector, connected to a Duo Expert LB 474 Evaluation Unit for signal processing. Circular lead shielding was placed around the pipe to confine radiation within the cross-section. Calibration was performed at ambient conditions using the known densities of air (1 kg m^{-3}) and water (997 kg m^{-3}), in accordance with manufacturer protocols.

A transparent optical window (Saint-Gobain Crystals) provided real-time visual access to the internal flow. This 7-inch pipe segment, made of sapphire crystal to withstand high temperature and pressure, was secured in a steel housing at the end of the test pipe. A high-speed camera (IDS Imaging) recorded the internal flow through the sapphire tube at rates of up to 350 frames per second.

The orifice insert and acoustic emission (AE) probe are used to conduct cavitation tests. Cavitation is induced by driving the fluid through the orifice, where a localized pressure drop promotes vapor bubble formation. As these bubbles collapse, they emit high-frequency acoustic signals, which are detected by the AE probe. These measurements can provide insight into cavitation intensity, dynamics, and spatial distribution. However, the detailed analysis of cavitation behavior and AE signal interpretation lies outside the scope of this paper.

2.2 Operating procedures

Experimental conditions simulated geothermal-relevant environments, with temperatures up to 180 °C and pressures up to 25 bar, tested in both vertical and horizontal orientations. The working fluid composition ranged from pure water to brine solutions containing 3.5 or 11 wt.% NaCl, with either N_2 or CO_2 as the gas phase. Additionally, low-temperature experiments at 30 °C were conducted using water and N_2 to replicate the test conditions reported by Schmidt et al. (2008), enabling direct comparison between their results and the present study. The test conditions are summarized in Table 1.

Table 1. Summary of experimental conditions conducted in the Geo-loop

Fluid composition	Temperature, °C	Pressure, bar
H_2O-N_2	30	2-8
H_2O-N_2	100-180	10-25
H_2O-CO_2	60-180	10-25
H_2O-3.5wt%NaCl-N_2	140-160	10-15
H_2O-3.5wt%NaCl-CO_2	140	15
H_2O-11wt%NaCl-CO_2	100-140	15-20

Upon loading the appropriate liquid phase, the setpoint temperature is entered in the control unit, which activates the reservoir heaters. The circulation pump is started to ensure uniform heating as fluid flows continuously through the loop. Once the desired temperature is reached, pressure is adjusted by introducing or venting N_2 or CO_2, followed by system stabilization.

When temperature and pressure are stable, multiphase flow experiments begin. A data logger records pressure, temperature, flow rate, and bulk density at 0.1-second intervals for two minutes, while high-speed video is captured for 5–10 seconds.

Each series starts with single-phase liquid flow. The gas-phase input is then increased stepwise by adjusting the flow control valve (Fig. 2b), allowing stabilization between steps. This continues until the pump nears its gas handling limit, after which pump speed is increased and the sequence restarts with pure liquid flow.

3. RESULTS AND DISCUSSION

3.1 Flow regime observation through optical cell

Figures 4 and 5 shows images of the flow inside the optical window during vertical upward and horizontal flow experiments of water and 3.5 wt.% NaCl brine as the liquid phase and N_2 and CO_2 as the gas phase. The figure shows the transition of flow regime with varying bulk gas volumetric fraction (C_G), calculated from the gas (Q_G) and liquid (Q_L) flow rates measured using the rotameter and ultrasonic flowmeter, respectively, following Equation 1.

$$C_G = \frac{Q_G}{Q_G + Q_L} \qquad (1)$$

Vertical upward flow experiments reproduced two distinct flow regimes as described by Taitel et al. (1980). At the start of each experiment (Fig. 4-1 and 4-5), the flow consisted of homogeneous liquid. When gas was introduced at low flow rates, small bubbles formed and moved randomly through the liquid phase (Fig. 4-2 and 4-6). As the gas fraction increased, these bubbles began to coalesce into larger bubbles (Fig. 4-3 and 4-7), eventually forming fully developed gas slugs (Fig. 4-4 and 4-8). These gas slugs, often

Proceedings 47th New Zealand Geothermal Workshop
11 -13 November 2025
Rotorua, New Zealand
ISSN 2703-4275

referred to as Taylor bubbles, occupy nearly the entire pipe diameter and exhibit a bullet-shaped or spherical nose.

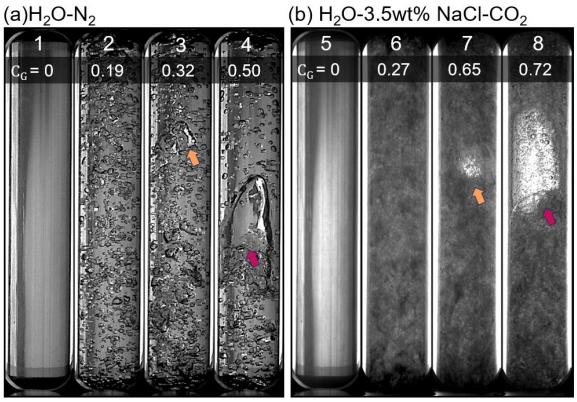

Figure 4. Vertical upward flow of (a) H_2O-N_2 and (b) H_2O–3.5 wt.% NaCl-CO_2 at 140 °C and 15 bar, showing the transition of flow regimes from homogeneous liquid (1,5), to bubble flow (2,6), to coalescing bubbles (3,7), indicated by the orange arrows, and finally to fully developed gas slugs (4,8), indicated by the red arrows.

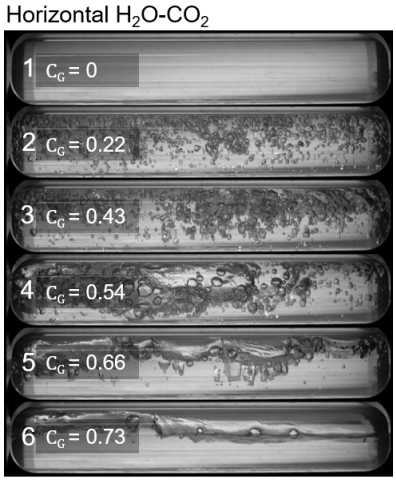

Figure 5. Vertical flow of H_2O-CO_2 at 140 °C and 15 bar, showing the transition of flow regimes with increasing gas content, from homogeneous liquid (1), to bubble flow (2), to coalescing bubbles (3), to elongated gas slugs (4), to intermittent separated flow (5), and finally to fully developed stratified wavy flow.

Similarly, horizontal flow experiments demonstrated three distinct flow regimes, as described by Taitel and Dukler (1976). Beginning with a pure liquid phase showing homogeneous flow (Fig. 5-1), the introduction of a small gas content resulted in bubble flow dispersed throughout the liquid (Fig. 5-2). As the gas content increased, these bubbles began to merge (Fig. 5-3), eventually forming elongated gas slugs (Fig. 5-4). Further increasing the gas content, the slugs combined and intermittently formed separated gas–liquid layers (Fig. 5-5), which ultimately developed into a stratified wavy flow pattern (Fig. 5-6).

These results demonstrate the system's capability to visualize flow regimes under a range of conditions, including variations in temperature, pressure, and fluid composition. Compared to transparent PVC, glass, or acrylic tubes commonly used in earlier multiphase flow studies (Sutton et al., 2006; Schmidt et al., 2008; Affonso et al., 2020), the sapphire optical window provided the necessary robustness to withstand the higher temperatures and salinity levels representative of geothermal systems.

The experiments also highlight a key limitation in the current design of the Geo-loop, specifically, the maximum gas flow rate that can be achieved. The pump, acting as the sole driver of circulation, experiences gas locking beyond a certain gas fraction, which limits the range of flow regimes that can be studied. Plans are already in place to address this by installing a gas compressor that would drive gas phase flow. This would not only increase the maximum gas ratio, but would also enable separate control of gas and liquid flow rates. This modification could facilitate future investigation of additional flow regimes, such as churn and annular flow.

3.2 Bulk density measurements and void fraction calculation

Figure 6 presents a comparison between the measured density of water, heated from 60 °C to 140 °C, obtained using the gamma densitometers, and the theoretical densities calculated from the equation of state for H_2O (Wagner & Pruß, 2002). The results show deviations of less than 0.7%, demonstrating the reliability of the gamma densitometers across a wide temperature range. Furthermore, these measurements were taken externally without disrupting the flow, unlike the quick-closing valve method (e.g., Godbole et al., 2011), which requires abruptly stopping the flow, or capacitance sensors (e.g., Maldonado et al., 2024), which require inserting a wire mesh into the pipe.

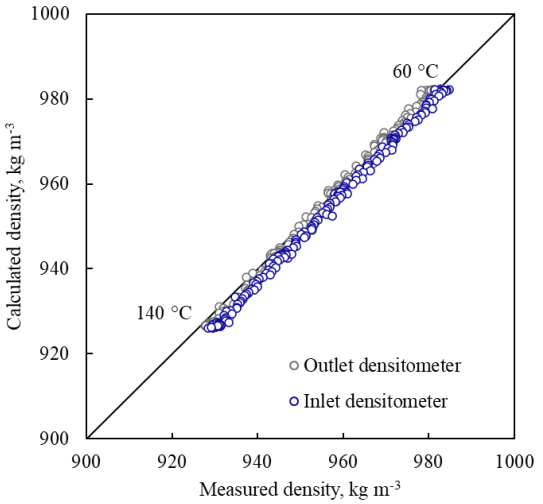

Figure 6. Density measurements of single-phase liquid water heated from 60 to 140 °C, obtained using gamma densitometers and compared with theoretical values calculated from the Equation of State for H_2O from Wagner and Pruß (2002).

The gamma densitometers were also used to measure the bulk densities of multiphase flows. Figure 7 shows results from two H_2O-N_2 flow experiments: one at 25 °C and 8 bar, and the other at 180 °C and 15 bar. Each experiment began with single-phase liquid flow, followed by a gradual increase in the gas volumetric fraction. In both cases, the results

ISSN 2703-4275

reveal a decrease in bulk density with increasing gas content, demonstrating the densitometers' ability to capture density variations in dynamic multiphase systems.

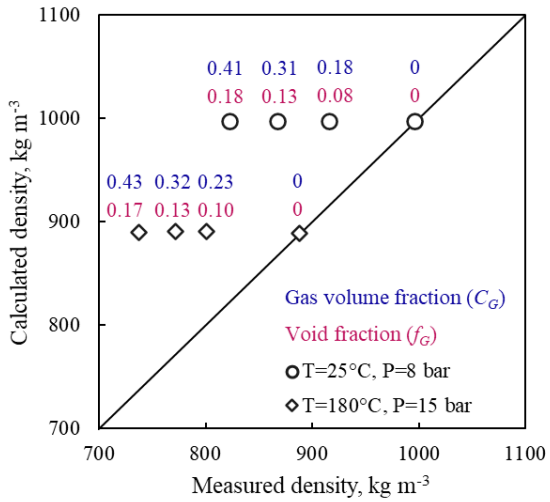

Figure 7. Density measurements for H_2O–N_2 multiphase flows, showing a decrease in bulk density with increasing gas volume fraction (C_G). Corresponding calculated void fractions (f_G) are also presented.

Bulk density measurements enable the calculation of the bulk velocities of each phase. The proportion of the cross-sectional area occupied by the gas phase, referred to as the void fraction, is related to the bulk density of the flow (ρ_m), as expressed in Equation 2. The theoretical densities of the gas (ρ_G) and liquid (ρ_L) phases can be determined using established equations of state.

$$\rho_m = f_G \rho_G + (1 - f_G)\rho_L \qquad (2)$$

In both examples shown in Figure 7, the calculated void fractions are significantly higher than the gas volumetric fractions, indicating that the gas phase travels much faster than the liquid phase. This highlights the capability of the flow loop to characterize the relative velocities of phases in multiphase flows.

3.3 Benchmarking with another experimental setup and existing multiphase correlations

The data collected from the Geo-loop are compared with multiphase data obtained using a different experimental setup. Schmidt et al. (2008) used a flow loop to investigate the effect of fluid viscosity on void fraction. Their published results include experiments with H_2O–N_2 at 20 °C, which were readily replicated using the Geo-loop. These data, combined with those from the present study, were then evaluated against existing multiphase flow correlations, for example, the Duns and Ros (1963) correlation, which is widely used in wellbore simulators such as SwelFlo (McGuiness, 2015), and Gudrun (Franz and Clearwater, 2021), and the Rouhani and Axelsson (1970) model, used in FloWell (Gudmundsdottir et al., 2013).

Figure 8 compares the measured void fractions from Schmidt et al. (2008) for H_2O–N_2 and the Geo-loop H_2O–N_2 data at a similar temperature of 30 °C with the modeled void fractions predicted by the Duns and Ros (1963) correlation. Both datasets show reasonable agreement with the model, indicating that the Duns and Ros correlation can effectively predict void fraction under these conditions. In contrast, the Geo-loop H_2O–N_2 data at a higher temperature (140 °C) and the brine (3.5 wt% NaCl)–N_2 data at 140 °C deviate significantly from the model predictions.

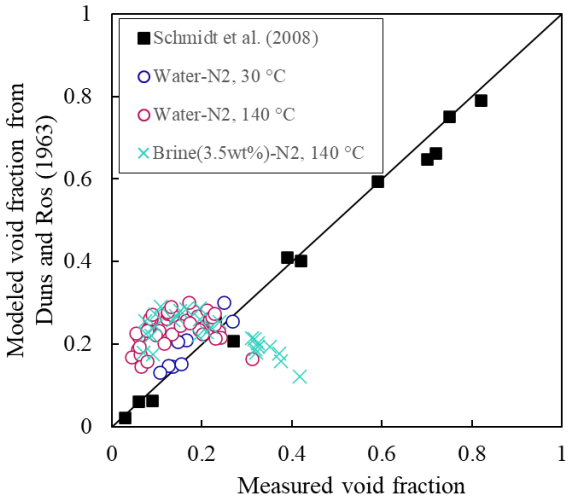

Figure 8. Comparison of void fraction measurements from Schmidt et al. (2008) and Geo-loop multiphase experiments with void fractions modeled using the Duns and Ros (1963) correlation.

The same analysis is presented in Figure 9, this time using the drift-flux model developed by Rouhani and Axelsson (1970). The model also successfully predicts the experimental void fractions from the Geo-loop at low temperatures, as well as the data from Schmidt et al. (2008) at low void fractions. However, the high-temperature H_2O–N_2 data and the brine (3.5 wt% NaCl)–N_2 experiments show significant deviations from the model predictions.

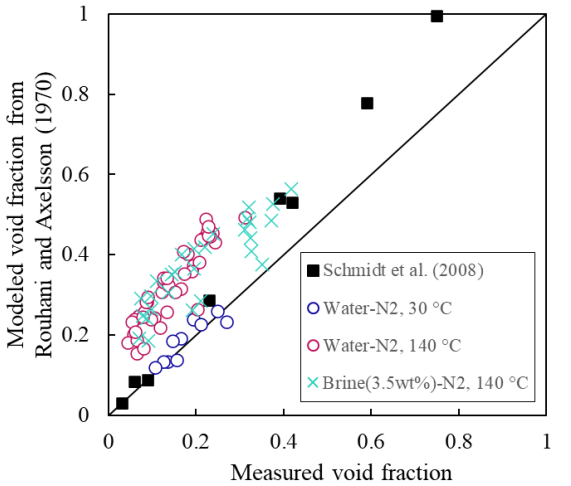

Figure 9. Comparison of void fraction measurements from Schmidt et al. (2008) and Geo-loop multiphase experiments with void fractions modeled using the Rohani and Axelsson (1970) drift flux model.

Figures 8 and 9 illustrate the Geo-loop's capability to replicate the experimental data of Schmidt et al. (2008) under

comparable temperature and composition conditions. This indicates that the Geo-loop provides reliable void fraction measurements in multiphase flow experiments. Additionally, the results support the applicability of the Duns and Ros (1963) and Rouhani and Axelsson (1970) models at low temperatures and salinities.

Figures 8 and 9 also show deviations between the measured void fractions and the predictions of the models at higher temperatures and in brine-dominated liquid phases, suggesting that the models do not adequately account for such conditions. This highlights the need to further investigate the effects of temperature and salinity and to incorporate these factors in multiphase flow models. The Geo-loop could serve as a platform to collect data under these conditions and support the development of more appropriate models.

4. CONCLUSIONS

The results demonstrate that the Geo-loop can effectively conduct multiphase flow experiments at temperatures up to 180 °C and with simulated brine containing up to 11 wt% NaCl. These conditions exceed those of many previous experimental setups that have traditionally been used to develop multiphase flow models that are still extensively used in wellbore and pipeline simulations. The results discussed in Sections 3.1 and 3.2 indicate that Geo-loop enables detailed investigations of two critical aspects of multiphase flow, specifically flow regime and void fraction.

The results presented in Section 3.3 show that the Geo-loop effectively replicates data from an independent flow-loop, reinforcing its reliability for multiphase flow experiments. Additionally, data collected at low temperatures using water –N_2 show agreement with predictions from two commonly used multiphase flow models. However, comparisons at elevated temperatures and salinities reveal potential inaccuracies, likely due to applying the models beyond the conditions under which they were originally developed. This highlights the need to critically evaluate current models and to develop new correlations specifically designed for geothermal conditions.

This work establishes the foundation for future studies by our team on geothermal fluid flow dynamics. Building on these findings, subsequent research will focus on refining multiphase flow models to better reflect geothermal reservoir conditions, including high-temperature, high-salinity environments.

ACKNOWLEDGEMENTS

This project received funding from European Union's Horizon 2020 under Grant Agreement #851816 (GeoPro) and Horizon Europe under Grant Agreement #101058163 (CRM-Geothermal). The authors would also like to thank colleagues from the University of Iceland, TWI, Flowphys, and other consortium partners in the GeoPRO project for their assistance in constructing the Geo-loop.

REFERENCES

Affonso, R. R. W., Dam, R. S. F., Salgado, W. L., Silva, A. X., & Salgado, C. M. (2020). Flow regime and volume fraction identification using nuclear techniques, artificial neural networks and computational fluid dynamics. Applied Radiation and Isotopes, 159, 109103. https://doi.org/10.1016/j.apradiso.2020.109103

AL-Dogail, A. S., & Gajbhiye, R. N. (2021). Effects of density, viscosity and surface tension on flow regimes and pressure drop of two-phase flow in horizontal pipes. Journal of Petroleum Science and Engineering, 205, 108719. https://doi.org/10.1016/j.petrol.2021.108719

Alvarez, R. R., & Cinco, F. R. (2011). Use of Wellbore Simulation as a Tool to Evaluate Well Issues in Mature Geothermal Fields. In GRC Transactions, Vol. 35.

Duns, H., & Ros, N. C. (1963). Vertical flow of gas and liquid mixtures in wells. In Proceedings 6th World Petroleum Congress (pp. 451–465). Frankfurt.

Godbole, P. V., Tang, C. C., & Ghajar, A. J. (2011). Comparison of void fraction correlations for different flow patterns in upward vertical two-phase flow. Heat Transfer Engineering, 32(10), 843–860. https://doi.org/10.1080/01457632.2011.548285

Gokcal, B., Wang, Q., Zhang, H.-Q., & Sarica, C. (2008). Effects of high oil viscosity on oil/gas flow behavior in horizontal pipes. SPE Projects, Facilities & Construction, 3(02), 1–11. https://doi.org/10.2118/102727-pa

Grant, M. A., & Bixley, P. F. (2011). Geothermal Reservoir Engineering, Second Edition. Elsevier: Academic Press.

Hasan, R., & Kabir, S. (2018). Fluid flow and heat transfer in wellbores. SPE.

Hewitt, G. F., & Yadigaroglu, G. (2017). Modelling strategies and two-phase flow models. Introduction to Multiphase Flow, 39–77. https://doi.org/10.1007/978-3-319-58718-9_2

Kabigting, N. V., Alvarez, R. R., & Menzies, A. J. (2021). Use of Pressure-Temperature-Spinner Surveys to Characterize Geothermal Production Well Behavior. In Proceedings World Geothermal Congress 2020+1. Reykjavik, Iceland.

King, T. R., Freeston, D. H., & Winmill, R. L. (1995). A Case Study of Wide Diameter Casing for Geothermal Systems. https://doi.org/10.2172/895960

Kumara, W. A. S., Halvorsen, B. M., & Melaaen, M. C. (2010). Single-beam gamma densitometry measurements of oil–water flow in horizontal and slightly inclined pipes. International Journal of Multiphase Flow, 36(6), 467–480. https://doi.org/10.1016/j.ijmultiphaseflow.2010.02.003

Libert, F., & Alvarez, R. (2015). Performance Analysis and Stimulation of Dry Steam Wells in Mak-Ban Geothermal Field, Philippines. In Proceedings World Geothermal Congress 2015. Melbourne, Australia.

Lv, X. F., Gong, J., Li, W. Q., Shi, B. H., Yu, D. & Wu, H. (2013). Experimental study on natural-gas-hydrate-slurry flow. SPE Journal, 19(02), 206–214. https://doi.org/10.2118/158597-pa

Maldonado, A. D., Rodrigues, C. C., Mancilla, E., dos Santos, E. N., da Fonseca Junior, R., Marcelino Neto, M. A., da Silva, M. J., & E. M. Morales, R. (2024). Spatial distribution of void fraction in the liquid slug in vertical gas-liquid slug flow. Experimental Thermal and Fluid Science, 151, 111093. https://doi.org/10.1016/j.expthermflusci.2023.111093

Márquez-Torres, L., Ochoa-Pineda, J., Pico, P., Valdés, J. P., Becerra, D., Pinilla, A., Pereyra, E., & Ratkovich, N. (2020). Comparison of 63 different void fraction correlations for different flow patterns, pipe inclinations, and liquid viscosities. SN Applied Sciences, 2(10). https://doi.org/10.1007/s42452-020-03464-w

Orkiszewski, J. (1967). Predicting two-phase pressure drops in vertical pipe. Journal of Petroleum Technology, 19(06), 829–838. https://doi.org/10.2118/1546-pa

Ribeiro, J. X. F., Liao, R., Aliyu, A. M., Baba, Y. D., Archibong-Eso, A., Ehinmowo, A., & Zilong, L. (2020). An assessment of gas void fraction prediction models in highly viscous liquid and gas two-phase vertical flows. Journal of Natural Gas Science and Engineering, 76, 103107. https://doi.org/10.1016/j.jngse.2019.103107

Rouhani, S. Z., & Axelsson, E. (1970). Calculation of void volume fraction in the subcooled and quality boiling regions. International Journal of Heat and Mass Transfer, 13(2), 383–393. https://doi.org/10.1016/0017-9310(70)90114-6

Schmidt, J., Giesbrecht, H., & van der Geld, C. W. M. (2008). Phase and velocity distributions in vertically upward high-viscosity two-phase flow. International Journal of Multiphase Flow, 34(4), 363–374. https://doi.org/10.1016/j.ijmultiphaseflow.2007.10.013

Taitel, Yehuda, Barnea, D., & Dukler, A. E. (1980). Modelling flow pattern transitions for steady upward gas-liquid flow in vertical tubes. AIChE Journal, 26(3), 345–354. https://doi.org/10.1002/aic.690260304

Taitel, Yemada, & Dukler, A. E. (1976). A model for predicting flow regime transitions in horizontal and near horizontal gas-liquid flow. AIChE Journal, 22(1), 47–55. https://doi.org/10.1002/aic.690220105

Tonkin, R. A., O'Sullivan, M. J., & O'Sullivan, J. P. (2021). A review of mathematical models for geothermal wellbore simulation. Geothermics, 97, 102255. https://doi.org/10.1016/j.geothermics.2021.102255

Vestøl, S., Kumara, W. A. S., & Melaaen, M. C. (2017). Gamma densitometry measurements of gas/liquid flow with low liquid fractions in horizontal and inclined pipes. International Journal of Computational Methods and Experimental Measurements, 6(1), 120–131. https://doi.org/10.2495/cmem-v6-n1-120-131

Wagner, W., & Pruß, A. (2002). The IAPWS formulation 1995 for the thermodynamic properties of ordinary water substance for general and scientific use. Journal of Physical and Chemical Reference Data, 31(2), 387–535. https://doi.org/10.1063/1.1461829

Yadigaroglu, G., & Hewitt, G. F. (2018). Introduction to multiphase flow: Basic concepts, applications and modelling. Springer.